World Journal of Pharmaceutical Science and Research
www.wjpsronline.com
Review Article
ISSN: 2583-6579
SJIF Impact Factor: 3.454
Year - 2024
Volume: 3; Issue: 2
Page: 132-160

TO STUDY THE DESIGN AND BIOPHARMACEUTICAL EVALUATION OF NANOPARTICLES CONTAINING 5-FLUOROURACIL (5-FLUORO-H,3-H-PRIMIDINE2,4-DIONE)

Raveendran K. C.*

Nehru College of Pharamcy, Pampady, Thrissur, Kerala India.

Article Received: 29 January 2024 | | Article Revised: 15 February 2024 | | Article Accepted: 07 March 2024

Corresponding Author: Raveendran K. C.
Nehru College of Pharamcy, Pampady, Thrissur, Kerala India.
DOI: https://doi.org/10.5281/zenodo.10946303

ABSTRACT

Cancer is a major public health concern in both developed and developing countries. Now a days, the treatments of cancer categorizes in to 5 classes, Surgery, Radiation, Chemotherapy, targeted and immunotherapy. Cancer chemotherapy is one the major way to treat cancer without medical assistants. The main aim of the ideal cancer chemotherapy is to deliver the correct amount of drug with desired controlled rate and sufficiently longer duration of time to the site of action (Tumor cells) to obtain the desired therapeutic response. Traditional cancer chemotherapy is based on the promise that tumor cells are more likely to be killed by anticancer drugs because of the faster proliferation of those cancer cells. However, in reality most of the drugs cannot differentiate cancer cells from the normal cells. This results in the undesirable effect of the drug because of the lack of selectivity. To minimize this risk, the development of tumor targeted drug delivery systems of anti-cancerous agents is necessary. The success of therapy depends on the selection of ideal carriers' system that can deliver the drug selectively to tumor cells. These carries include nanoparticles, nanotubes, nanorods, dendrimers, micelles, solid lipid nanoparticles, microspheres.

KEYWORDS: Tumor cells, nanoparticles, nanotubes, nanorods, dendrimers, micelles, solid lipid nanoparticles, microspheres.

INTRODUCTION

WHO reported that Cancer is one of the leading cause of morbidity and mortality world -wide with 14 million cases approximately in 2012.According to the Union for international Cancer control (UICC), over 7 million people die of Cancer, and more than 11 million new cases are diagnosed world-wide. In next two decades, it is expected to be raise the number of new cases to about 70%, It was reported that cancer is responsible for 8.8 million death in 2015.Cancer is a major public health concern in both developed and developing countries. Now a days, the treatments of cancer categorizes in to 5 classes, Surgery, Radiation, Chemotherapy, targeted and immunotherapy. Cancer chemotherapy is one the major way to treat cancer. The aim of the ideal cancer chemotherapy is to deliver the correct amount of drug

with desired controlled rate and for sufficiently longer duration of time to the site of action (Tumor) cells, while prevent the normal cells to obtain the desired therapeutic response.

A nanoparticle is a particle having the size range of 1-1000 nm in dimension. The 5-Flurouraci l(5-Fluoro-1 H,3H-pyrimidine-2,4-dione) is a known earlier antineoplastic, antimetabolite. All the materials used in the experiments were of analytical grade. The optimization of individual material were done The 5-FU was found that the in-vivo drug release of 5-FU from BPEI-PLGA NPs at pH 7.4 and pH 5 was best explained by Higuchi's Model, as the plot showed the highest linearity with the regression coefficient of 0.989 and 0.990 respectively. It was found that the in-vivo drug release of 5-FU from BPEI-PLGA NPs at pH 7.4 and pH5 was best explained by Higuchi's Model, as the plot showed the highest linearity with the regression coefficient of 0.989 and 0.990 respectively.

5-FLUOROURACIL (5-FLUORO-H,3H-PYRIMIDINE-2,4-DIONE)

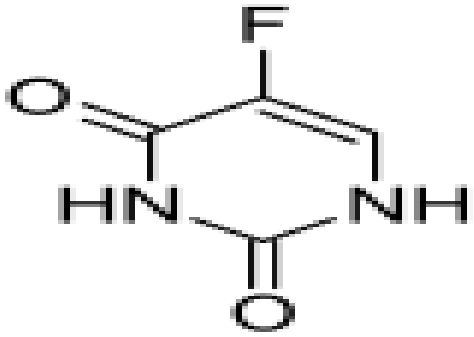

Figure 1: Chemical structure of 5-Fluorouracil.

Description

Empirical formula: C4H3FN2O2**, CAS number** is 51-21-8, **Molecular weight** 130. 077223 g/mol, **IUPAC name**: 5-Fluoro-1 H,3H-pyrimidine-2,4- dione **Category:** Anti-neoplastic, antimetabolite, Pyrimidine analogu5-Fluorouracil is a white to nearly white crystalline powder, Practically odorless.

Melting point: **282 - 283º C**

Solubility: 1 gm in 80 ml;170 ml Ethyl alcohol & 55 ml methanol; practically insoluble in chloroform, ether & benzene; solubility in aqueous increases with increase pH of solution.

Mechanism of action

5-FU requires enzymatic conversion to the nucleotide status (ribosylation and phosphorylation) to exert its cytotoxic activity. Several routes are available for the formation of fluoxuridine monophosphate(FUMP). Uridinephosphorylase converted 5-FU to fluorouridine and then to Floxurine monophosphate by uridine kinase, or it may be react directly with 5-phosphoribosyl- 1 – pyrophosphate(PRPP), catalyzed by orotate phosphor ribosyl transferase, to form FUMP.

Further, metabolic pathways are available to FUMP as the triphosphate FUTP, it is incorporated in to RNA. In an alternative reaction sequence crucial for antineoplastic activity, it is reduced to FUDP by ribonucleotide reductase(RNR) to the deoxynucleotide level and forming of FdUMP. 5-FU may also be converted by thymidine phosphorylase to the deoxy riboside fluoro-deoxy uridine(FUdR) and then by thymidine kinase to FdUMP, a potent inhibitor of thymidylate synthetase(TS), FdUMP inhibits TS and blocks the synthesis of TTP, a necessary constituent

of DNA. The folate co-factor Methylene-tetrahydrofolate and FdUMP form a covalently bound ternary complex with TS. This inhibited complex resembles the transition state formed during the enzymatic conversion of dUMP to thymidylate. The physiological complex of TS folate-dUMP progresses to the synthesis of thymidylate by transfer of the methylene group and two hydrogen atoms from folate to dUMP, but this reaction is blocked in the inhibited complex of TS-FdUMP-folate by the stability of the fluorine carbon on FdUMP; sustained inhibition of the enzyme results.

Pharmacokinetics

Intravenous administration of 5-FU produces peak plasma concentration of 0.1-0.5 µM, plasma clearance is rapid(with a $t_{1/2}$ of 10-20 minutes). Only 5-10% of a single intravenous dose of 5-FU is excreted intact in the urine. Given by continuous intra venous infusion for 24-120 hours,5-FU achieves steady state concentrations range of 0.5-0.8 µM.5-FU enters the CSF in minimal amounts.

PLGA

PLGA is approved by FDA and European Medicine Agency in drug delivery systems for parenteral administrations. PLGA is a synthetic copolymer of lactic acid(α –hydroxyl propionic acid) and glycolic acid(α-hydroxy acetic acid).lactic acid contains an asymmetric carbon and therefore has 2-optical isomers. They are (+) lactic acid and D(-) lactic acid. Lactic acid contains in all living organism and is the intermediate or end product of carbohydrate metabolism. In vivo degradation of PLGA leads to the formation of harmless products. Final degradation products are lactate(salt of lactic acid) and glycolate(salt form of lactic acid).

Polyethyleneimine as cat-ionic polymer

PEI is a polymer that has been used for common processes such as paper production, shampoo manufacturing and water purification. Two types of polymers are available: Linear and branched. The branched type is formed by cationic polymerization of Azirudine monomers, via chain growth mechanism for gene therapy. The branched form of PEI contains 1º, 2º and 3ºamines, each with a potential to be protonated. This gives PEI the attribute of serving as an effective buffer through a wide pH range .With nitrogen appearing as one out of every three atoms in the PEI backbone, any benefits of branching and proton-ability quickly accumulate in relation to the overall polymer size.

Use of Biotin as targeting ligand:-Biotin is a water soluble vitamin generally classified with the B-complex also known as vitamin B7 or coenzyme R. Biotin is composed of a ureido (tetra-hydroimidazolone) ring fused with a tetrahydrothiophene ring. At the cellular level biotin act a growth promoter and works as a coenzyme for carboxylase enzymes in the preparation of fatty acids, isoleucine and valine and participates in gluconeogenesis. Biotin plays a key role in cell signaling, epigenetic gene regulation and chromatin structure.

EXPERIMENTAL INVESTIGATION

The aim of the study was to Design and Development of Nanoparticle containing the drugs. The Pharmacodynamics Properties were Optimized and Evaluated by using modern techniques like FTIR, U.V-Vis Spectroscopic methods, Zero potential determination for particle size determination etc. conducted. Before that each drugs and excipients were optimized individually as well as their formulation. Again the properties of the formulation after loading the drug also evaluated. The properties of the drugs and stability studies of formulations establish the complete the profile of the formulation.

CHARACTERIZATION OF 5- FLUOROURACIL

FTIR spectroscopy

The FTIR spectra of 5-fluorouracil was obtained and shown in annexure 8.1. Spectrum was examined for the presence of any characteristic peaks. It shows peaks of N-H stretching at 3200 cm^{-1},C- O Stretch and C-N stretch at 1650 cm $-^{1}$,C-H bending (in plane) at 1250 cm^{-1},C-O at 1200 cm^{-1}. The result observed was in close agreement with reported data.

UV –spectrophotometry

The UV- spectrum of 5-FU in water, PH 5 phosphate buffer and pH 7.4 phosphate buffer saline showed characteristic peak at 266 nm. The result observed was in close agreement with reported data.

UV spectra of 5 FU in water

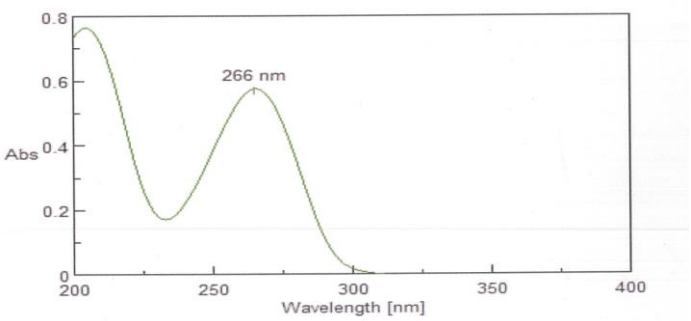

UV spectra of 5-FU in pH 5 phosphate buffer

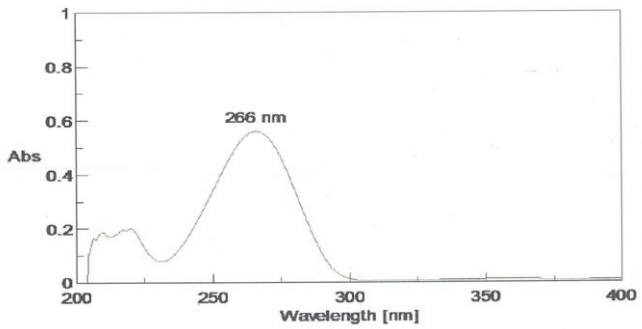

UV spectra of 5-FU in pH 7.4 phosphate buffer

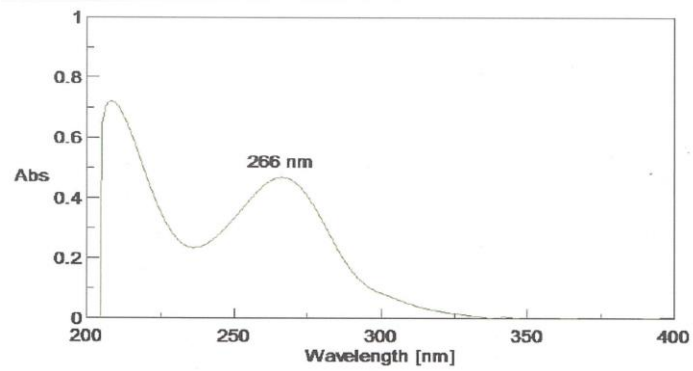

UV - Calibration curve calibration plot of 5-FU in water

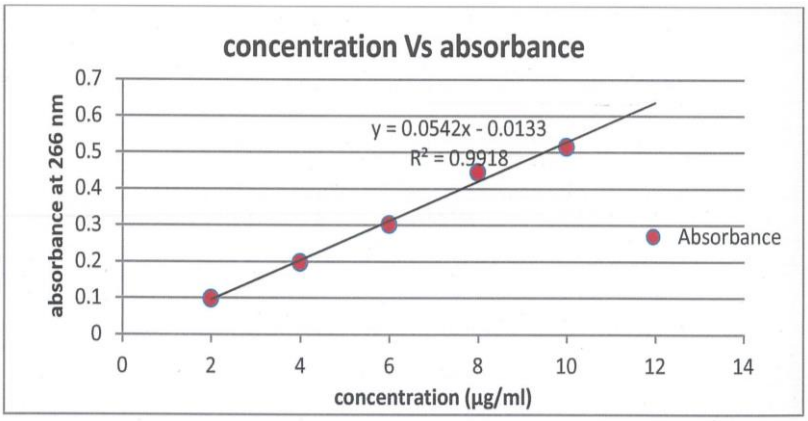

UV calibration curve in pH5 phosphate buffer

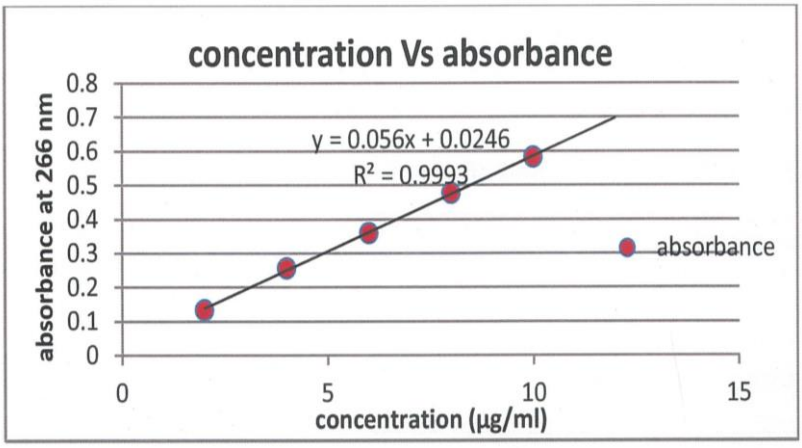

UV-calibration curve in pH 7.4 PBS

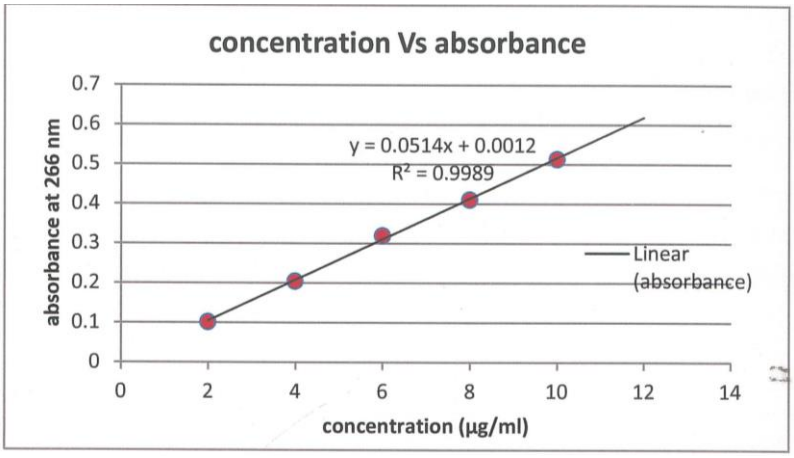

Figure: Calibration plot of 5-Fluorouracil in pH7.4.PBS

Differential Scanning Calorimetric

The DSC data of 5-FU was obtained and shown in annexure. It was examined for the presence of any characteristic peaks. A sharp endothermic peak appears between 281 -286 ºC which corresponds to the melting transition of 5 –FU

Powder X-ray Diffraction

The powder X-ray diffraction pattern of 5 –FU was obtained. It shows characteristic peaks at 28.1º,33.5º,18.5º,20º and 21.3º which were intense and sharp indicates its crystalline nature.

Melting point

The melting point of 5 – FU was found to be in the range of 282 - 284ºC The result observed was close agreement with reported data.

CHARACTERIZATION OF PLGA

Solubility

PLGA was found to soluble in dichloromethane, chloroform, Dimethyl form amide and DMSO.

FTIR Spectroscopy:- The FTIR spectra of PLGA was recorded and shown in annexure. Spectrum was examined for any characteristic peaks. It shows characteristic peaks of ester group at 1753 cm^{-1} due to C –O stretching, C-O bending band at 1188 cm^{-1},characteristic peaks of CH3 group at 2988 cm^{-1} due to stretching vibrations of C-H and 1454 cm^{-1} due to C-H bending. The result was in close agreement with reported data.

Differential Scanning Calorimetry:-The DSC data of PLGA was obtained and shown in annexure. It was examined for the presence of any characteristic peaks. A mild endothermic peak appears between 30 -50 ºC which corresponds to the glass transition of PLGA.

Powder X-ray Diffraction:- The powder X-ray diffraction pattern of PLGA was obtained and shown in Annexure . No peak was observed for PLGA which indicates that PLGA is an amorphous co-polymer.

CHARACTERIZATION OF BRANCHED POLYETHYLENEIMINE

FTIR Spectroscopy:-The FTIR spectra of PEI was recorded and shown in annexure. Spectrum was examined for any characteristic peaks. It shows characteristic peaks of primary Amine at 3453 cm^{-1} due to N–H stretching, N-H bending band at 1600 cm^{-1}, characteristic peaks of secondary Amine at 3315 cm^{-1} due to stretching vibrations of N-H and characteristic peaks of C-H_2 at 1459 cm^{-1} due to C-H bending. The result was in close agreement with reported data.

UV spectrophotometry:- The Spectrum of PEI in water was showed in figure

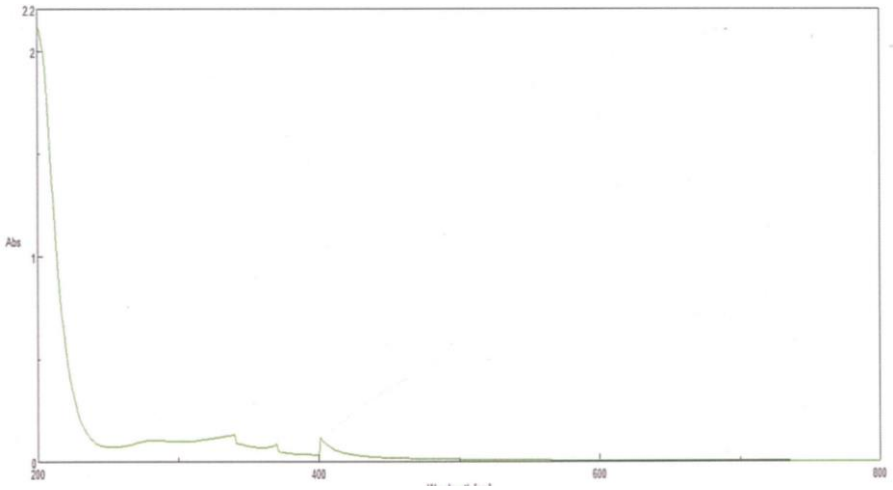

U. V. Spectrum of PEI in water

CHARACTERIZATION OF D- BIOTIN

FTIR Spectroscopy:-The FTIR spectra of biotin was recorded and shown in annexure. Spectrum was examined for any characteristic peaks at 1706 cm^{-1} due to C–O stretching, N-H stretching at 3393 cm^{-1}, characteristic peaks of carboxylic O-H bending at 3024 cm^{-1}, C –O band at 1271 and characteristic bands of C-S at 650 cm^{-1}. The result was in close agreement with reported data.

UV Spectrophotometry:-The UV Spectrum of Biotin in water was shows a characteristic absorption at far UV region.

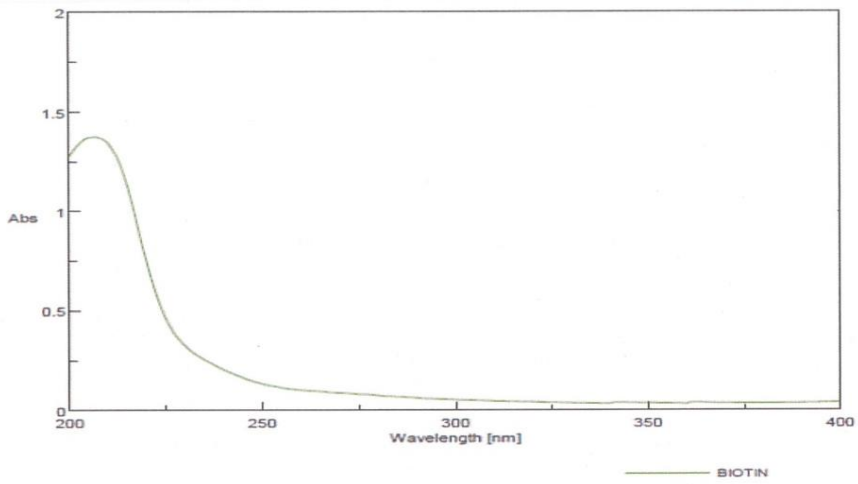

Melting point:-The melting point of biotin was found to be in the range of 231 -233ºC. The result observed was in close agreement with reported data.

DRUG -EXCIEPIENT COMPATIBILITY STUDIES

FTIR Spectroscopy

PLGA -5 –FU mixture:-The FTIR spectra of PLGA- 5FU was recorded and shown in annexure. Spectrum was examined for the characteristic peaks of 5- FU and PLGA ,C –O group of amide and carboxylic acid overlap to form a broad peak, at 3310 cm^{-1} due to N–H stretching, C-F stretching at 1098 cm^{-1}, C-O band of ester group of PLGA at 1271 cm-1, O-H bending at 3103 cm^{-1}. The spectrum shown that there is no interaction with 5 –FU and PLGA.

5-FU – PEI mixture:-The FTIR spectra of 5-FU – PEI was recorded and shown in annexure C-O stretching of 5-FU at 1732cm-1,N-H bending at 1631 cm^{-1}, C-F stretch at 1027 cm^{-1},N-H stretch of primary amino group with amide N-H stretch, peak formed at 3464cm $-^{1}$.FTIR spectrum gives individual peaks of 5-FU and PEI, so the spectrum suggest that there no interaction with 5-FU and PEI.

Differential Scanning Colorimetry

DSC of PLGA -5-FU mixture:-The DSC data of PLGA- 5-FU was obtained and shown in annexure . It was examined for the presence of characteristic sharp endothermic peak of 5-FU appears between 281 -286 ºC. This data suggest that there is no interaction with 5-FU and PLGA.

PRE-OPTIMIZATION STUDY FOR THE PREPARATION OF PLGA NANOPARTICLES

The various factors which may affect the particle size of the formulation were understood in pre-optimization study. The particle size was found to depend up on PVA concentration time, sonication time, volume of outer phase(PVA solution). Further relationship of the particle size of PLGA NPs could be established by optimization process.

Preparation of PLGA nanoparticles

Nanoparticles(NPs) were prepared by double emulsification(W1/O/W2) solvent evaporation technique. It involves 2 major steps,

1. The formation of stable droplets of the primary emulsion and the removal of solvent from the droplets of secondary emulsion. 50 mg of PLGA was dissolved in a mixture of Dichloromethane(2ml) and acetone (2ml).Then add ultrapure water(1 ml) to the PLGA solution followed by ice water sonication for 2 minutes to form primary emulsion(W1/O).
2. The primary emulsion was added drop-wise to 0.5% PVA solution(20ml) under stirring at 1500 rpm. White color secondary emulsion(W2/O) was formed. Thus formed emulsion was sonicated for 30 min. the emulsion was mechanically stirred for overnight to allow the evaporation of organic solvent. Filter the NP suspension through cellulose nitrate membrane0.8 µm, The NPs were collected by centrifugation at 6000 rpm for 15 minutes. Washing thrice with ultrapure water and then freeze dried to obtain NPs as dry powder.

OPTIMIZATION OF PREPARATIONOF PLGA NPs

Optimization of nanoparticles was carried with central composite statistical design with 3 factors, 5 levels and 20 runs was selected for the study design using Design Expert 10.0.2 software trial version (state –Ease inc, Minneapolis, (USA).This design is suitable for exploring quadratic response surfaces and constructing second order polynomial models.

BC	8109.01	1	8109.01	16.45	0.0023	
A^2	43431.52	1	43431.52	88.99	<0.0001	
B^2	24859.32	1	24859.32	50.42	<0.0001	
C^2	3452.26	1	3452.26	7.00	0.0245	
Residual	4930.26	10	493.03			
Lack of Fit	4034.58	5	806.92	4.50	0.0621	Not significant
Pure Error	895.68	5	179.14			
Cor Total	1.856E+005	19				

The Model F-value of 40.71 implies that the model is significant. The “Pred – R-Squared of 0.8228 is in reasonable agreement with the “ADJ R-squared” of 0.9495; i.e, the difference is less than 0.2, Adeq Precision” measure the signal to noise ratio. A ratio greater than4 is desirable. Ratio of 25.199 indicates an adequate signal. This model can be used to navigate the design space.

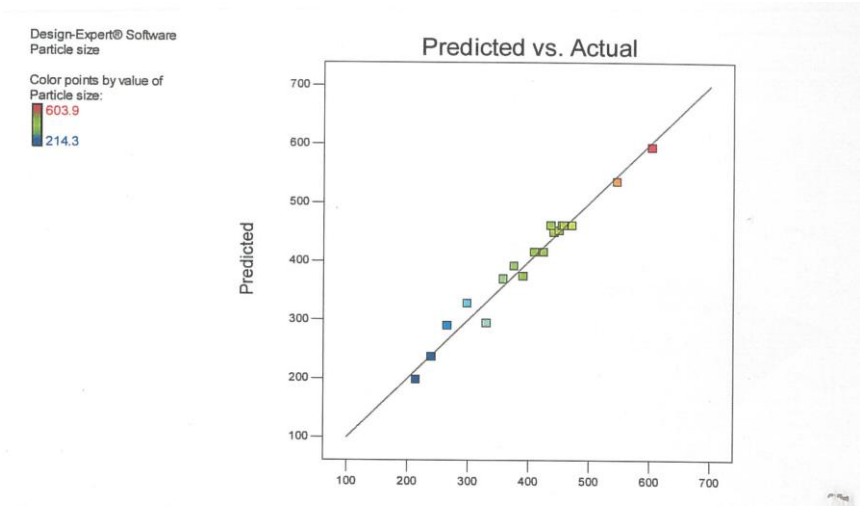

ANOVA graph of predicted value v/s Actual value

This model proposed the following the following polynomial equation in terms of coded factors for particle size of PLGA NPs.

R1 = 461 +40.87A + 29.00B +53.13C +42.81AB + - 41.91AC +31.84BC +-54.90 A^2 +-41.53 B^2 +15.48 C^2

Where R1is the particle size, A is the concentration of PVA solution is the sonication time and C is the Volume of outer Phase.

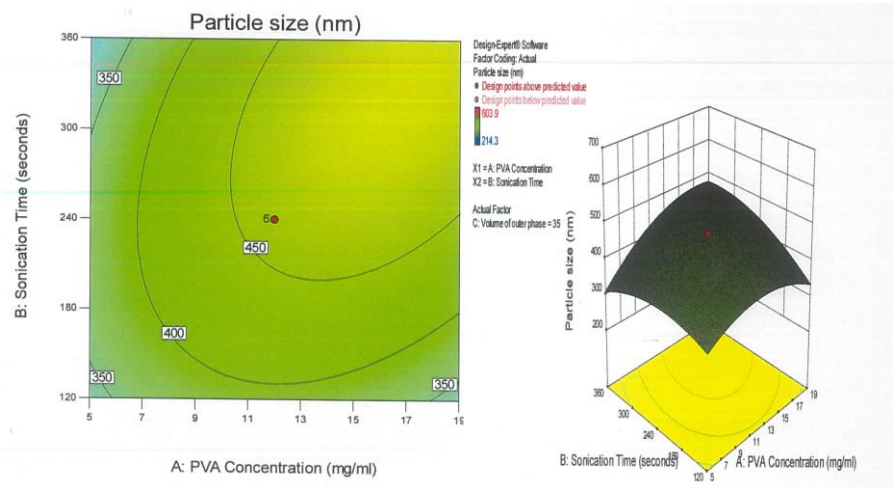

Figure: Contour plot of particle size of PVA solution.

Optimized formula

The Optimized formula was determined after studying the effect to find dependent variables on responses. The criteria followed for generating the optimized formula based on selecting the individual Variable and defining their goal and limits. The table gives the optimization Constraints selected for reaction variable. After defining constraints for each variables, Design Experts software ®automatically generated the optimized formula. In Table gives the optimized Formula generated by Design Expert software® showing the predicted and the experimental Values obtained. It was observed that the percentage prediction error was low (3.51%) which indicates the accuracy of the prediction by the software and the utility of the experimental design for process optimization.

Optimization Constraints selected for optimization of PLGA NPs

Variables	Constraints		
Independent variables	**Lower limit**	**Upper limit**	**Goal**
A = Concentration of PVA solution	5	19	In range
B = Sonication time	120	360	In range
C = Volume of outer phase	15	55	In range
Dependent variables			
R1 = particle size	214.3	603.9	minimize

Table: Predicted and experimental values obtained based on optimized formula for preparation of PLGA NPs.

Predicted values based on Optimized formula			
Factors			Responses
Concentration of PVA solution(mg/ml)	Sonication time (seconds)	Volume of outer phase(ml)	Particle size (nm)
5.00894	348.988	15.0182	210.3
Experimental values based on optimized formula			
Factors			
Concentration of PVA solution(mg/ml)	Sonication time (seconds)	Volume of outer phase(ml)	Particle size (nm)
5.00894	348.988	15.0182	217.7
Percentage Prediction error			3.51

CHARACTERIZATION OF PLGA NPS

FTIR Spectroscopy

FTIR spectrum of PLGA- NPs was obtained and shown in Annexure. Chemical composition of the nanoparticle surface were evaluated by FT-IR spectroscopy bands are formed at 1759(C=O stretch), 1084(C-O stretch),CH,CH2,CH3 stretching vibrations between 2850 –2950, OH stretching around 3059.

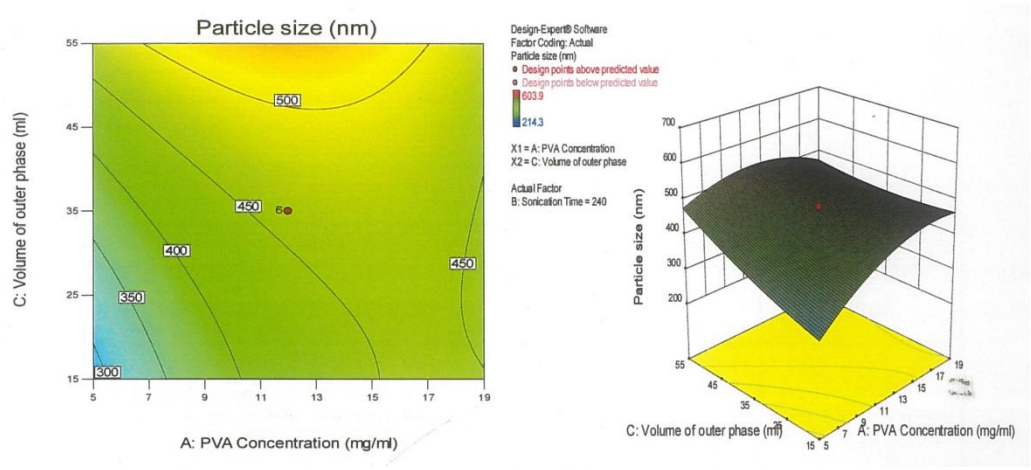

Contour plot and response surface plot of factor a v/s B against particle size of PLGA nanoparticle

Mean particle size

The average diameter of the optimized PLGA NPs was found to be 217.7 nm. The Result Quantity was good. From which it was confirmed that the PLGANPs have uniform size distribution.

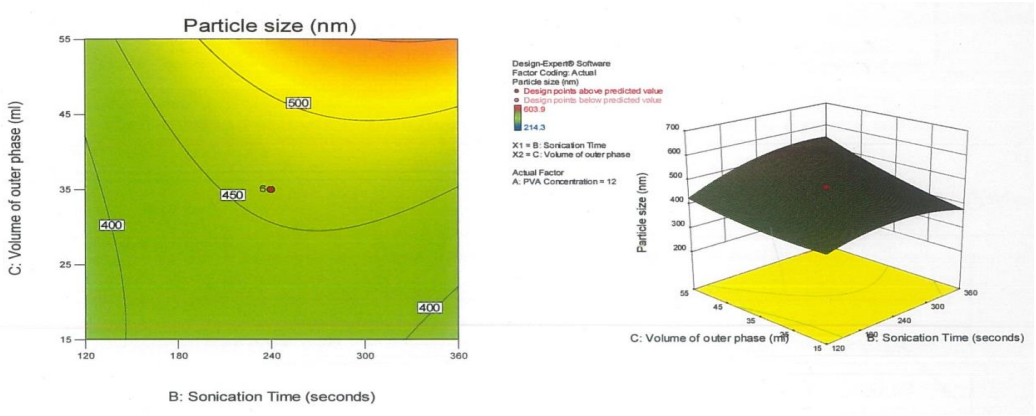

Contour plot and response surface plot of factor A v/s B against Mean particle size of PLGA nanoparticle

Mean zeta potential

The mean zeta potential value obtained is -20.0. The result quality was good so it could be said that zeta potential was uniform distributed. The negative zeta potential value was attributed to the carboxylic acid groups present on the surface of PLGA NPs.

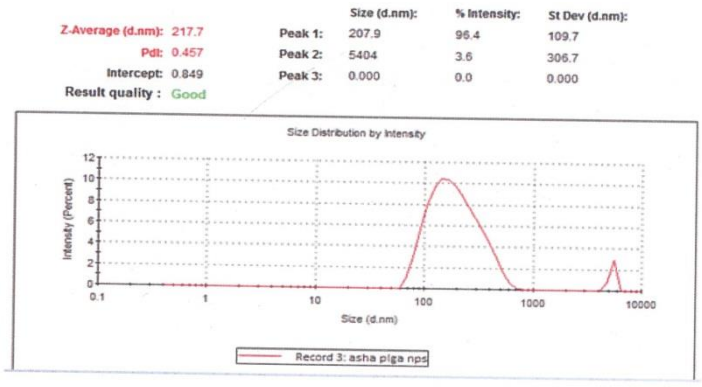

Figure: Particle size of PLGA nanoparticles.

Scanning Electron Microscopy

SEM images of optimized was shown in figure .The figure indicated that the nanoparticle have spherical shape and uniform size distribution.

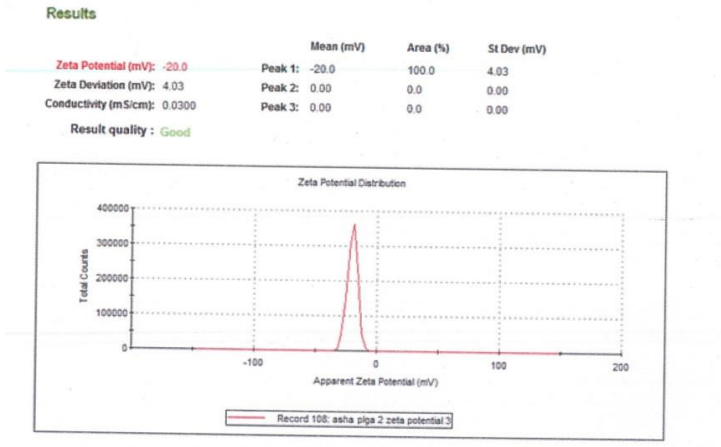

Figure: Mean Zeta potential of PLGA Nanoparticle.

Transmission electron Microscopy

The TEM images confirms the spherical shape and uniform size distribution of the optimized PLGANPs. The particle size observed in TEM images was in reasonable agreement with the size of the nanoparticle size analyzer.

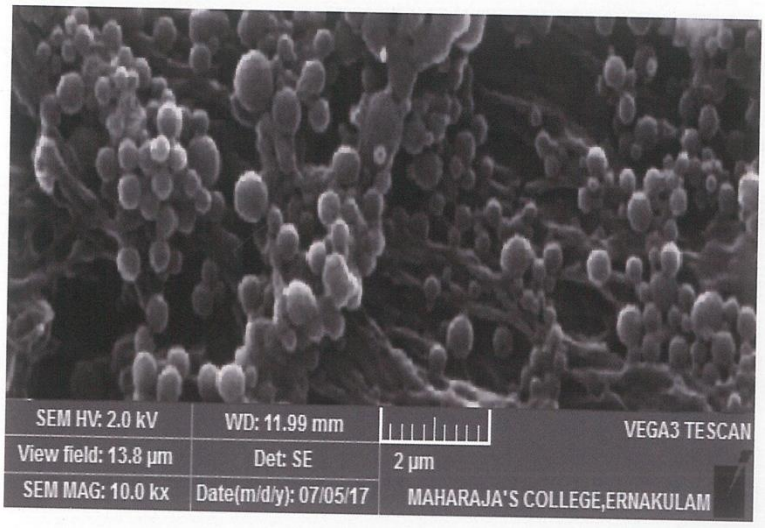

Figure: Scanning Electron Microscopy of PLGA Nanoparticle.

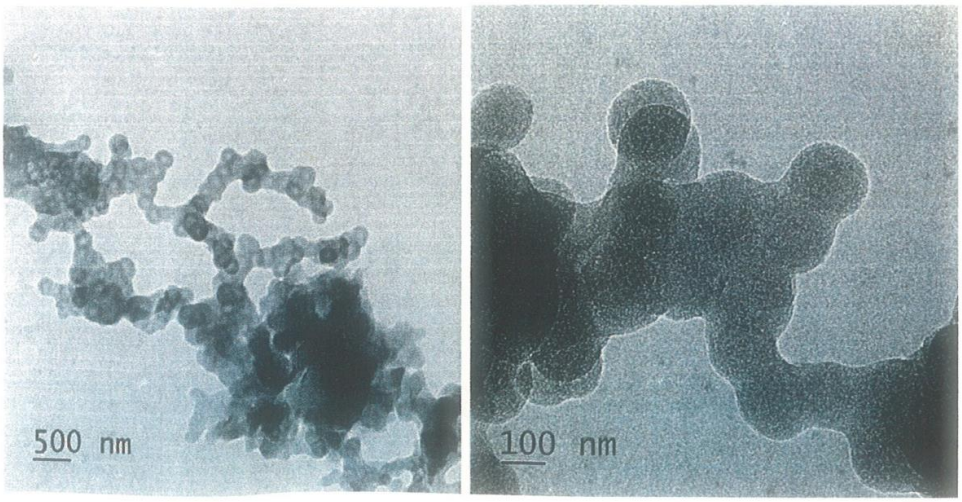

Figure: Transmission Electron Microscopy of PLGA NPs.

IN-VITRO HEMOLYSIS ASSAY OF PLGA NPs

Hemolysis assay of PLGA NPs was conducted with different concentrations and results were tabulated in the table.

Figure showing Hemolysis Assay of PLGA NPs.

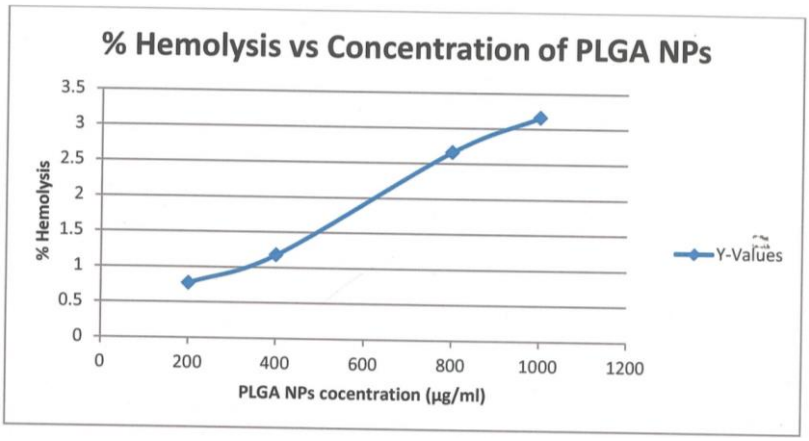

Figure: Plot of percentage Hemolysis by PLGA-NPs.

The hemolysis activity of PLGANPs was dose dependent. The percentage hemolysis increases with increase in concentration of PLGA NPS. But the hemolytic activity of PLGA NPs was found to be feasible.

DRUG LOADING

Drug loading was done with the optimized formulation for the preparation of PLGA nanoparticle.

- **Mean particle size**:-Mean particle size was slightly increases from the optimized formula for blank PLGA NPs due to the encapsulation of drugs at the core of nanoparticles.
- **Mean zeta potential:-**It was observed that a slight increase in zeta potential of drug loaded PLGA NPs from the blank PLGA NPs. It may be due to the attachment of some of the drug at NPs surface during preparation.

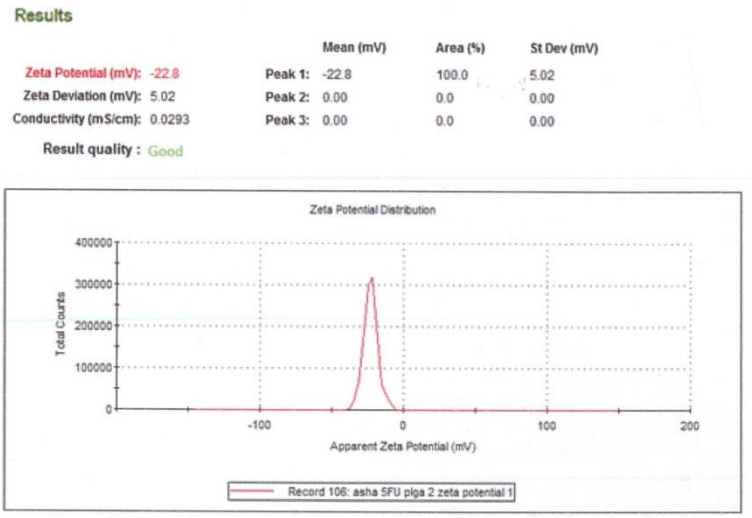

Figure: Mean zeta potential of Drug loaded PLGA-NPs.

Encapsulation Efficiency

The encapsulation efficiency of the PLGA NPS was defined as the percentage of 5-FU encapsulated in respect to the total amount of 5-FU used to prepare the PLGA NPs. The encapsulation efficiency was determined by indirect method and encapsulation efficiency was found to be only 65%.This may be attributed to the water soluble nature of 5-FU which lead to its rapid partitioning in to the aqueous phase and hence decreased encapsulation in to the nanoparticles during PLGA deposition.

Yield of nanoparticle

Yield of PLGA NPs was found to be 68%.

In - vitro drug release from PLGA NPs:- In –vitro release of 5-FU from PLGA NPs at pH 7.4 PBS (physiological pH) was determined. The profile for cumulative percentage drug release of 5-FU from PLGA NPs at pH 7.4 was shown in the table 6.9.5.The 5-FU that was adsorbed on the nanoparticle surface was firstly released during the first 6 hour (Initial burst release). After the initial burst release, a sustained drug release pattern was observed for PLGA NPs.

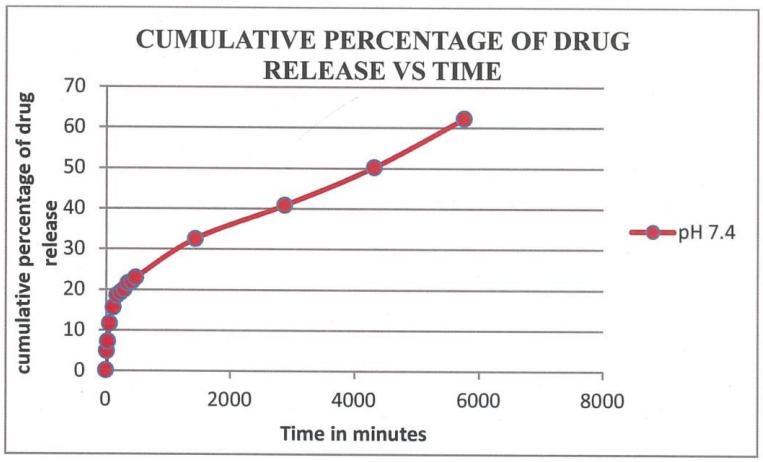

Figure: Cumulative percentage drug release from PLGA-NPs.

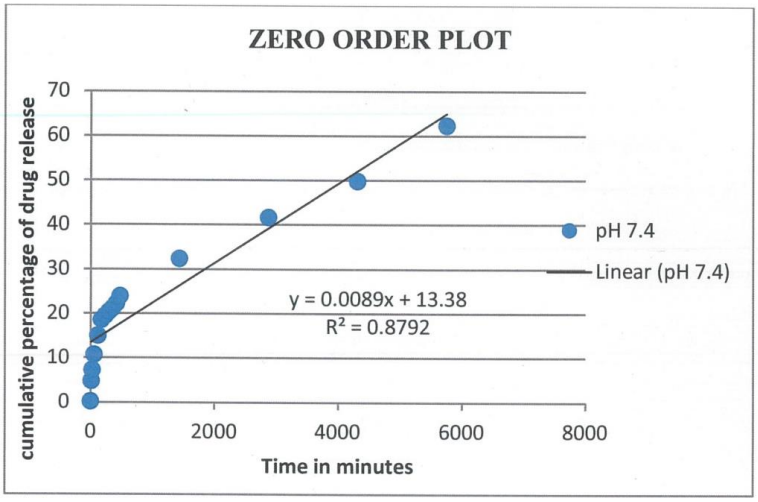

Figure: Zero order plot for PLGA-NPS.

It was found that the in vitro drug release of 5-FU from PLGA NPs at pH7.4 was best explained by Higuchi's Model, as the plot showed the highest linearity with the regression coefficient of 0.973 respectively. This explain why the drug diffuses at comparatively slower rate as the distance for diffusion increases, which is referred to as Higuchi's kinetics.

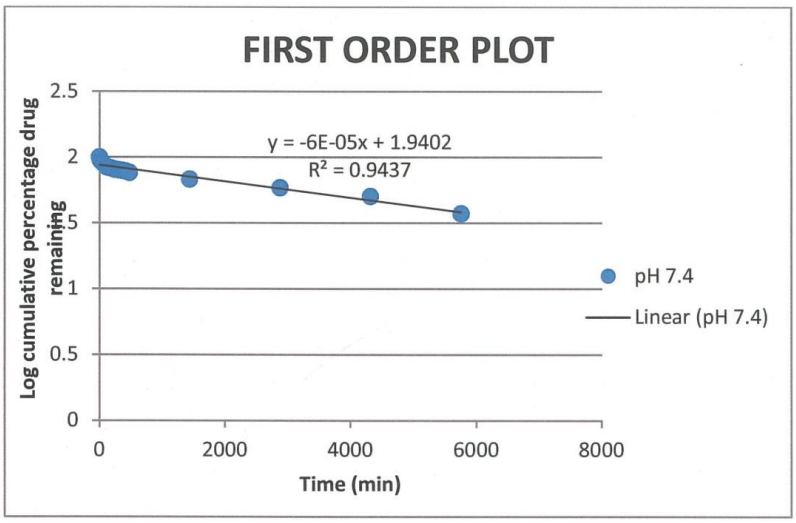

First order plot for PLGA-NPs

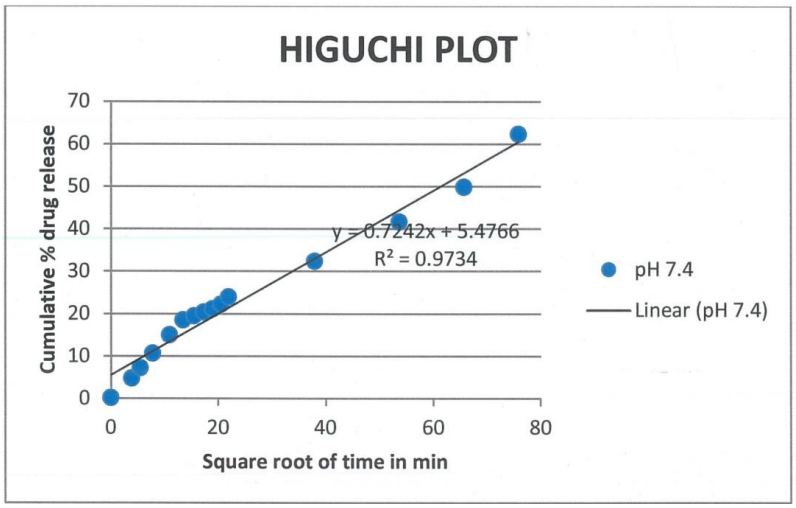

Higuchi plot for PLGA-NPs

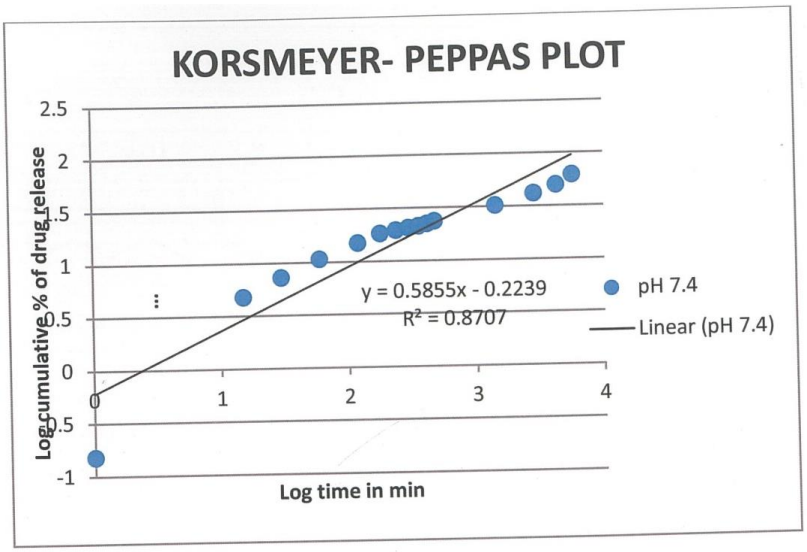

The Korsmeyer –peppas plot (log Cumulative percentage drug release vs. log time) indicated linearity at pH 7.4(R^2 =0.870) with n values 0.585 respectively. The Korsmeyer - peppas plot is used to determine the mechanism of drug release from a system. Here the obtained n values were between 0.43 and 0.85 which shows that the mechanism of release of 5-FU from PLGA NPs follows a non fickian or anomalous diffusion.

SYNTHESIS OF BIOTINYLATED POLYETHYLENEIMINE (BPEI)

Biotin was conjugated to branched polyethyleneimine for the preparation of BPEI. Biotin (30 mg) was activated with NHS (14 mg) and EDC (23mg) in dimethyl sulfoxide (3ml). The activated biotin solution was added to 25KDa PEI(200mg) in de-ionized water(12 ml). The reaction mixture was stirred at 20 ^{0} C for 24 hrs. As formed biotinylatepolyethylineimine was purified by dialyzed against water for 2 days(MWCO:8000 -12000).Purified product was lyophilized and defined as biotinylatedpolyethyleneimine(BPEI).

FTIR spectroscopy:-FTIR spectrum of BPEI was obtained and given in the annexure 8.13, absence of OH peak of biotin in the range of 2500 - 3000 cm $^{-1}$ reveals the conjugation of biotin to PEI. Peak at 1638 due to C- O stretch,3423 cm-1 and 1561 cm-1 due to NH stretch and bend .Peak at 614 cm-1 due to C–S group. Peaks at 2955 cm-1 and 2846 cm-1 due to asymmetric and symmetric stretching of CH group .Presence of characteristic peaks confirmed the conjugation of biotin to PEI.

H NMR spectroscopy:-The structure was confirmed proton NMR spectroscopy and the spectrum is shown in Annexure. The peaks of NH group at the fused ring of biotin and D_2O solvent overlap between ð4.5 and 5ppm in ^{1}H NMR spectra. The peaks between ð 2.3 -3.3 ppm shows the presence of hydrogen of carbon primary and secondary amino groups of PEI. The peaks below ð2 ppm belongs to hydrogen of carbon group present in the side chain of biotin. Peaks at ð7.9 ppm shows the presence of amide 'NH' clearly confirmed the conjugation of biotin to PEI

PREPARATION OF BIOTINYLATED POLYETHYLENEIMINE MODIFIEDPLGA NANOPARTICLES (BPEI-PLGA NPs) PLGA NPs surface was modified with biotinylated polyethyleneimine through EDC, NHS reaction.100 mg of freeze dried nanoparticles was dispersed in ultrapure water and add EDC(40mg) and NHS(20mg) for the activation of carboxyl group on the nanoparticle surface. After 4 hour add synthesized BPEI (60mg) to the activated PLGA NPs suspension, Stirred 24 hours. After 24 hour BPEI-PLGA NPS was centrifuged at 6000 rpm for 20 minutes, collected the nanoparticles and discard excess coupling reagent and un-conjugated BPEI in supernatant solution. Washed the BPEI-PLGA NPS thrice, freeze dried the product by using mannitol as cryoprotectant. Freeze dried BPEI-PLGA NPS was stored under 2-8 ºC.

Figure: Drug loaded loaded PLGA NPs.

CHARACTERIZATION OF BIOTINYLATED POLYETHYLENEIMINE MODIFIED NANOPARTICLES

FTIR spectroscopy:-FTIR spectrum of BPEI-PLGA NPs was obtained and given in the annexure .The spectrum shows characteristic peaks at 1759 cm-1 due to C- O stretch of PLGA,peak s at2928 cm-1 and 2854 cm-1 due to asymmetric and symmetric stretching of CH groups. Peak at 680 cm -1 due to C-S stretching of biotin. NH stretching bands formed in between 3100-3400 cm-1. Presence of characteristic peaks belongs to BPEI confirmed the surface modification on PLGA NPs.

Mean particle size:- The mean diameter of BPEI-PLGA NPs was found to be 275.8 nm .Surface modification with BPEI increase the mean diameter by 58nm.

Figure: Mean particle size of BPEI-PLGA NPs.

Mean zeta potential

Surface modification was clearly confirmed with zeta potential of BPEI –PLGA NPs .Zeta potential was found to be 24.1.Unmodified drug loaded PLGA NPs zeta potential was found to be -22.8.So the surface modification with BPEI reverse the surface charge from negative to positive zeta potential. In theory the more pronounced zeta potentials in the range of 20 -40 mV, being positive or negative, is favorable for stabilizing the nanoparticles in colloid solution. BPEI – PLGA NPs have zeta potential of 24 mV, so it stabilized the nanoparticles.

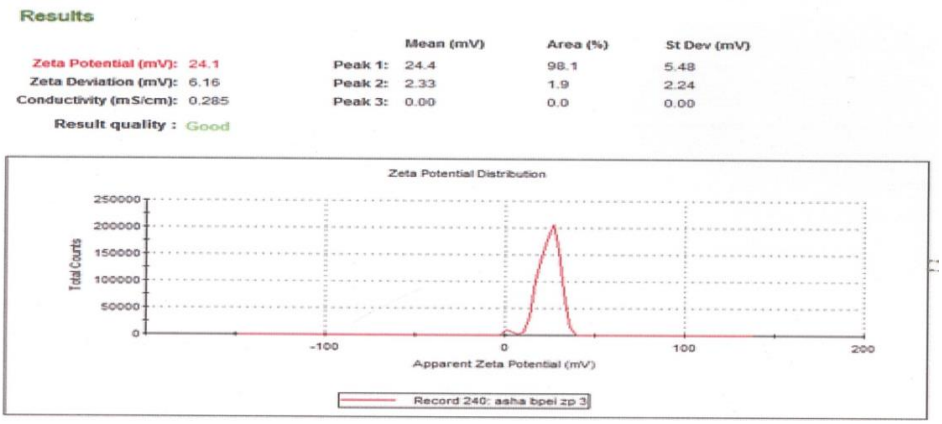

Figure: Mean Zeta potential of BPEI-PLGA-NPs.

Transmission Electron Microscopy:- Surface modification with BPEI maintained the spherical shape of PLGA NPs . The low density region in the image indicated the surface modification with BPEI. The BPEI-PLGA NPs was almost non disperse in nature. The particle size ranges obtained from dynamic light scattering were in consonance with that of TEM.

Determination of Encapsulation efficiency:- Encapsulation efficiency of 5-FU loaded BPEI_PLGA NPs was found to be 61%, Encapsulation efficiency was reduced from 65% to 61% due to small quantity of 5-FU leaked during surface modifications. However, the 5-FU leak might be favor to reduce the drug distribution on the surface layer of nanoparticles.

IN-VITRO HEMOLYSIS ASSAY OF BPEI –PLGA NPs

Hemolysis assay of BPEI-PLGA NPs was conducted with different concentrations and results were established in the **table.**

PLGA NPs Concentration (µg/ml)	Absorbance Of sample nm	Absorbance of positive control	Absorbance of negative control	% hemolysis	Mean ± SD
200	0.1307	1.7740	0.1077	1.38	1.37±0.0360
	0.1299			1.33	
	0.1311			1.40	
400	0.1367			1.74	1.93±0.1950
	0.1399			1.93	
	0.1432			2.13	
600	0.1531			2.72	2.74±0.2107
	0.1571			2.96	
	0.1501			2.54	
1000	0.1856			4.67	4.44±0.2040
	0.1811			4.40	
	0.1789			4.27	

Surface modification with BPEI slightly increases the hemolytic activity. The percentage hemolysis was found to increase only 1.3% at 1000µg/ml concentration. When compared to PLGA NPs.

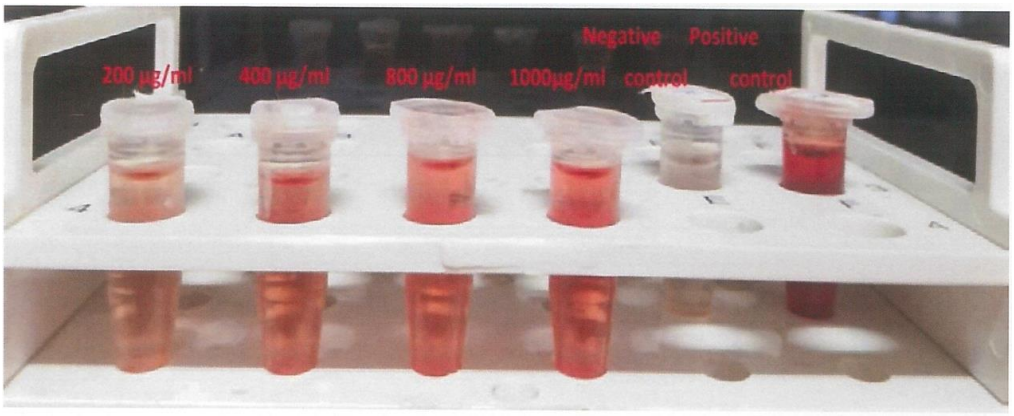

Figure. In –vitro hemolysis assay of BPEI-PLGA-NPs.

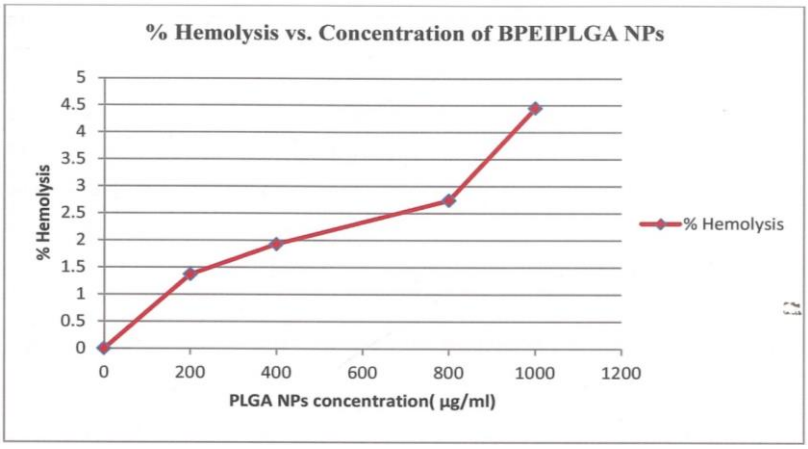

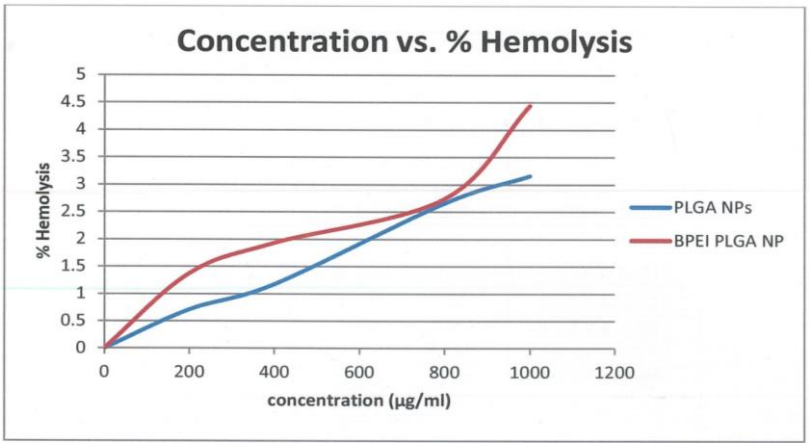

Figure. Plot of percentage hemolysis and effect of surface modification on percentage hemolysis by BPEI-PLGA-NPs.

IN-VITRO DRUG RELEASE STUDY OFBPEI –PLGA NPs

In vitro release of 5 –FU from PLGA NPs at pH 7.4 PBS(physiological pH) and pH 5 phosphate buffer (endosome pH of cancer cells) was determined. The profiles for cumulative per centage drug release of 5- FU from PLGA NPs at pH 7.4 and pH 5 are shown in the table. It was found that the initial burst release was reduced with surface modification. A sustained drug release pattern was observed and the amount of 5-FU released in pH 5 was higher than in pH7.4.The release of a drug from polymeric NPs is often modulated by different physicochemical parameters of the medium. BPEI layers surrounding PLGA NPs, whose amino groups are mostly protonated, dissolved in water, and therefore increase the release in acidic media.

Table. Regression Values of different drug release kinetics models for BPEI-PLGA NPs.

	Zero order	First order	Higuchi's	Korsmeyer peppas	
pH	R^2	R^2	R^2	R^2	n
7.4	0.942	0.964	0.989	0.985	0.492
5	0.890	0.945	0.990	0.982	0.490

From the table, it was found that the in-vivo drug release of 5-FU from BPEI-PLGA NPs at pH 7.4 and pH5 was best explained by Higuchi's Model, as the plot showed the highest linearity with the regression coefficient of 0.989 and 0.990 respectively. This explains why the drug diffuses at comparatively slower rate as the distance for diffusion increases, which is referred to as Higuchi' kinetics. The korsmeyer –peppas plot (log cumulative percentage drug release v/s log time) indicated linearity at pH 7.4 R^2 = 0.985 and pH 5(R^2 =0.982) with n values 0.492 and 0.490

respectively. The Korsmeyer –peppas plot is used to determine the mechanism of drug release from a system. Here the obtained n values were between 0.43 and 0.85 which shows that the mechanism of release of 5-FU from BPEI-PLGA NPs follows a non - flickian or anomalous diffusion. When compare with 5-FU release from modified nanoparticles, BPEI-PLGA NPs shows better control on drug delivery.

Cumulative percentage of drug release from BPEI-PLGA-NPs

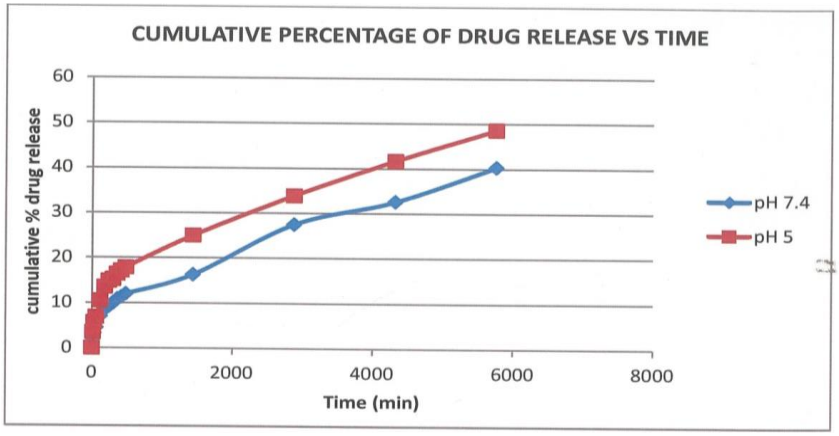

Figure: 6.32. Zero-order plot of BPEI-PLGA-NPs.

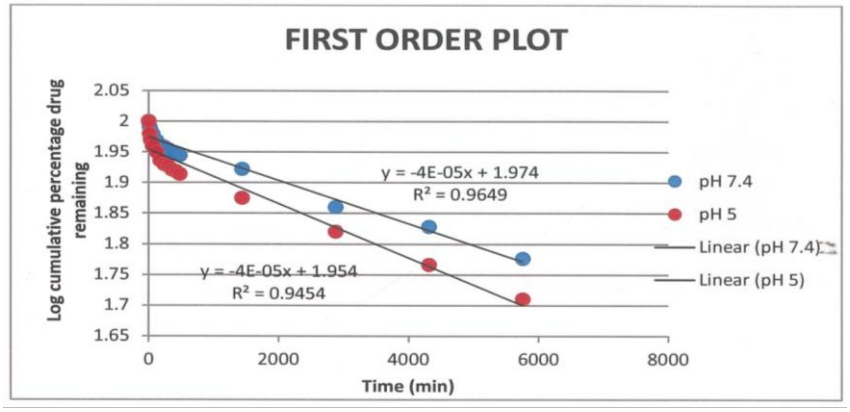

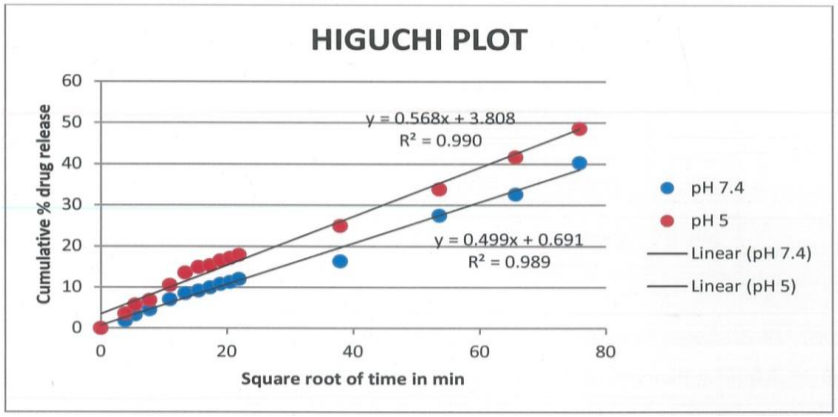

First order plot and Higuchi plot of BPEI-PLGA-NPs.

BRINE-SHRIMP LETHALITY ASSAY:- Brine shrimp lethality assay was carried out and percentage mortality of Artemia nauprii was determined.LC_{50}value was determined to find out the cytotoxic concentration. LC_{50}value was found out using probit analysis method. LC50 was found from log dose vs. probit value graph by interpolating probit

value 5, using equation from the graph(y= mx+c) The percentage mortality was found to increase with increase in concentration of PLGA-BPEI NPs(blank). An approximate linear correlation was observed when logarithmic concentration vs. Percentage mortality was plotted.LC 50 was found to be 831.76µg/ml.

Effect of different concentration of BPEI-PLGA NPs on percentage mortality of brine shrimp

Concentration in (µg/ml)	No. of brine shrimps	No. of dead Brine shrimps After 24 hrs.	No. of dead Brimeshrump After 24 hrs.	Percentage Mortality (%)
10	10	5	5	50
20	10	4	6	60
30	10	2	8	80
40	10	1	9	90
50	10	0	10	100
Negative control	10	10	0	0
Positive control	10	0	10	100

Table. Determination of probit value of BPEI-PLGA NPs.

Dose(µg/ml)	Log dose	Dead/Total	Percentage mortality	Corrected percentage	Probit value
10	1	5/10	50	50	5
20	1.3010	6/10	60	60	5.25
30	1.4771	8/10	80	80	5.84
40	1.6020	9/10	90	90	6.28
50	1.6989	10/10	100	97.5	6.8

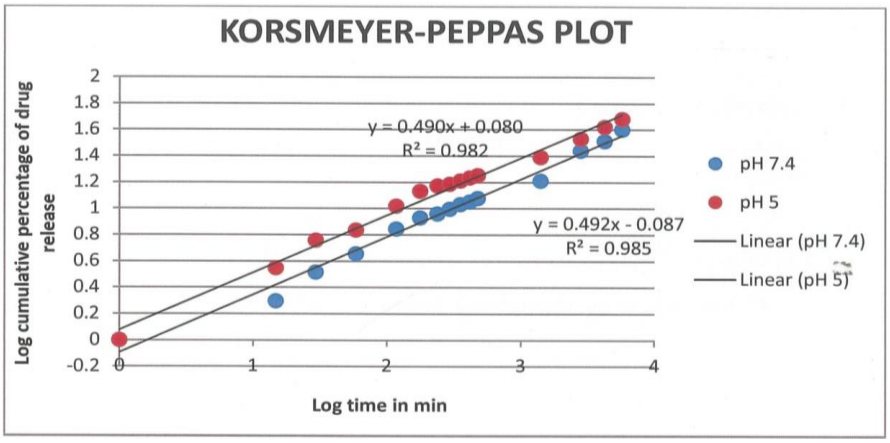

Figure. Korsmeyer-peppas plot for BPEI-PLGA-NPs.

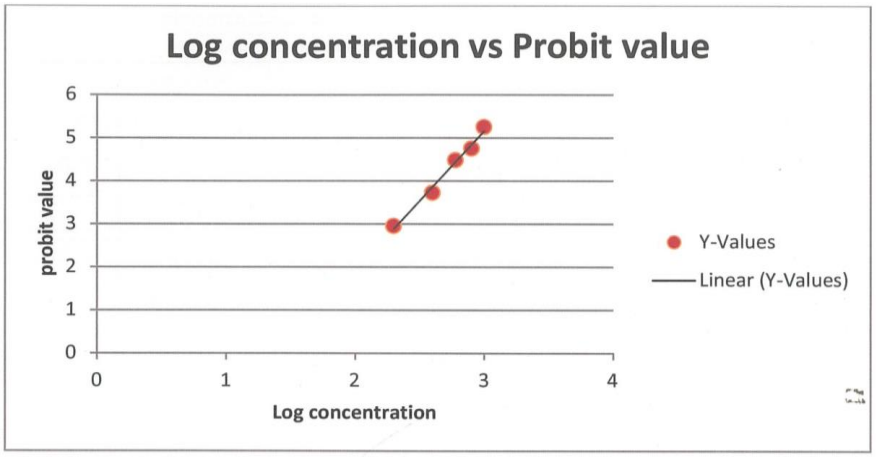

Plot of Drug dose vs. probit value of BPEI-PLGA_NPs.

The percentage mortality was found to increase with increase in concentration of PLGA-BPEI NPs(blank) .An approximate linear correlation was observed when logarithmic concentration vs. Percentage mortality was plotted.LC 50 was found to be 10µg/ml.

In –vitro cytotoxic assay

The in-vitro toxicity assessment of the prepared nanoparticles and free 5-FU was done on HeLa cell line and the data was tabulated below:

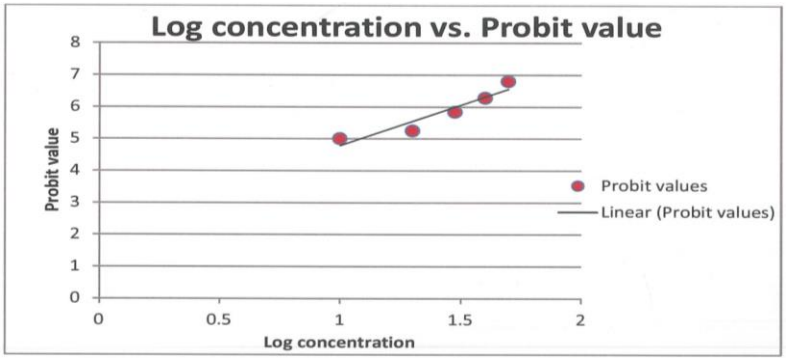

Plot of log concentration vs. probit value of BPEI-PLGA_NPs.

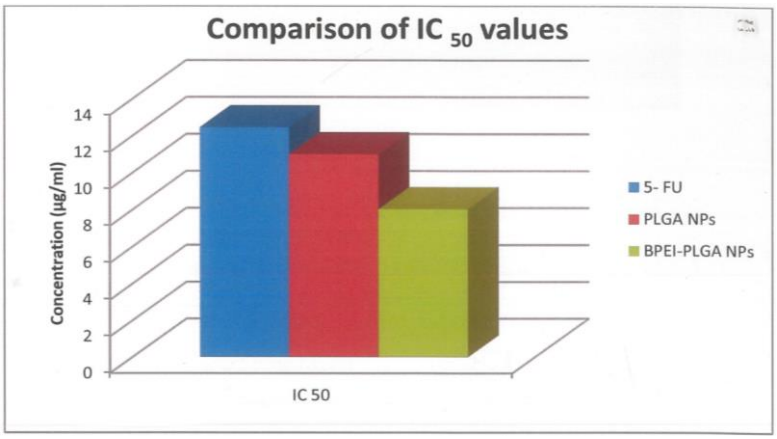

Comparison of IC50 of free 5-FU and nanoparticles.

Table. MTT assay of Free 5-FU.

Concentration of 5-FU (µg/ml)	Average optical Density of control at 540 nm	Average optical Density of test at 540 nm	Percentage validity
1.25	0.798±0.0130	0.697	87.46
2.5		0.621	77.81
5		0.533	66.79
10		0.403	50.50
20		0.261	32.7

MTT assay of BPEI-PLGA NPs.

Concentration of 5-FU (µg/ml)	Average optical Density of control at 540 nm	Average optical Density of test at 540 nm	Percentage validity
1.25	0.798±0.0130	0.658	82.45
2.5		0.581	72.80
5		0.472	59.14
10		0.299	45.44
2		0193	30.21

SUMMARY AND CONCLUSION

PLGA nanoparticles with 5-fluorouracil was prepared by double emulsification ($W_1/O/W_2$) solvent evaporation technique. 3.Optimized PLGA NPs was prepared and experimental value was obtained as 217.7, the percentage of prediction error was found to be 3.51%.The prepared PLGA nanoparticle was characterized by several methods. FTIR spectroscopy revealed the chemical structure of nanoparticle. Mean zeta potential was found to be negative ie,-20 mV, SEM image showed the spherical shape and uniform size distribution. The TEM image again confirmed the size and shape of PLGA NPs. PLGA NPs showed only 3% hemolysis at 1 mg/ml concentration. Drug loading was carried out with optimized formula. Encapsulation efficiency of Drug loaded PLGA-NPs is only about 65%. Drug loading slightly increase the particle size. Drug release from PLGANPs at pH 7.4 gives initial burst release followed by sustained release pattern. The drug release kinetics exhibited 5-FU loaded PLGA NPs found to follow Higuchi model with non-flickian anomalous diffusion mechanism .Ligand biotin was conjugated to cationic polymer polyethylineimine by using EDC and NHS chemistry and prepared biotinylated polyethylineimine. Biotinylation was confirmed with FTIR spectroscopy and 1H NMR spectroscopy. Surface modified PLGA NPs was prepared by conjugation of biotinylated PEI(BPEI-PLGANPS).Surface modification was confirmed by FTIR spectroscopy. The Mean particle size, Mean zeta potential and TE, FTIR spectroscopy confirms the surface modification. Surface modification was increased the particle size by 58.1 nm and reverse the surface charge from negative to positive(24.1). The BPEI coating was visible in TEM images. The hemolytic activity of BPEI-PLGA NPs was found to be 4.2% at 1mg/ml concentration.

Surface modification reduce the initial burst release, 5-FU showed at PH dependent release from BPEI-PLGA NPs which was showed in vitro drug release study. In vitro drug release at pH 5 was found to be more than pH 7.4.The release kinetics of BPEI-PLGA NPs was follow Higuchi model with non-Flickian anomalous diffusion. Surface modification provides a better control on drug delivery. Cytotoxicity of BPEI-PLGA NPs was studied by Brine shrimp lethality assay.LC50 value blank BPEI-PLGA NPs(blank) was found to be 831.76µg/ml and BPEI-PLGA NPs was found to be 10µg/ml. In vitro cytotoxicity studies was done by MTT assay on HeLa cell lines.IC_{50} values of the prepared nanoparticles found to be superior to free drug.

The BPEI-PLGA NPs have the greater cytotoxicity which might be attributed to the receptor mediated uptake of nanoparticles .Greater cellular uptake of BPEI-PLGA NPs might be due to the binding of the nanoparticles to biotin transport systems on the cell membrane of cancer cells. Cationic polymer coating increase the cell internalization by electrostatic interaction. MTT assay results shown that has no significant cytotoxicity. Finally from the above data it can concluded that BPEI-PLGA NPs can act as a tumor targeted drug delivery system.

REFERENCES

1. Zugagiotaj, Guedes C., Ponce S., Ferrer I., Molina – Pinela S., Paz-AresL, Current challenges in cancer treatment, Clin ther, 2016; 1-16.
2. Base Y.H, Park.K, targeted drug delivery to tumors: myths reality and possibility. J. control release, 2011; 153; 198-205.
3. Chen S. Zhao X,Chenj. KaznertsovaL, WongSS, Mechanism based tumor targeting drug delivery system.Validation of efficient vitamin receptor-mediated endocyosis and drug release, Bio conjugate Chem., 2010; 21: 979-987.

4. Kakdi D, Jain D, Shrivastava V, Kakdi R, Patil A.T, Cancer therapeutics opportunities, challenges and advances in drug delivery, Journal of applied Pharmaceutical sciences, 2011; 01(09): 01-10.
5. Nguyen T.K, Targeted nanoparticles for cancer therapy; promises and challenges, Nguyen j Nanomedic Nantechnol, 2011; 2(5).
6. Dharap S.S, Wang.Y, Chandana.P, Khandere J. J, Gunaseelan S, SinkoP. J, Tumor-specific targeting of an anticancer drug delivery system by LHRH peptide, PNAS, 2015; 102(36): 12962-12967.
7. Danhier F, Ansorena E, Silva J. M, coco R, Breton A. L, Preat V.A., PLGA based nanoparticles: an over view of biomedical applications, J. cornet, 2012; 161: 505-522.
8. Ruoslah E. Rajotte D, An address system in the vasculature of normal tissues and tumors. Annu. Rev. Immunol, 2000; 18: 813-827.
9. Ren WX, Hanj, Uhm S, Jang YJ, Kang C, Kim J. H., Recent development of biotin conjugation in biological imaging, sensing and targeted delivery. Chem Commun, 2015; 51(52): 10403-10418.
10. Gabizon A, Harowitz AT, GorenD, Tzemachd, Mandelbaum Shavit F, Qazen M M, et al., Targeting folate receptor with folate linked to extremities of poly(ethylene glycol)-grafted liposomes; in vitro studies, Biocojugate Chem, 1999; 10: 289-298.
11. Ishida O, Maryuma K, Tanahashih, Iwatsuru M, Sasaki H, Eriguchi M, Liposomes bearing polyethylene glycol coupled transferrin with intracellular targeting property to the solid tumors in vivo, Pharm Res., 2000; 1(18): 1042-1048.
12. FrankelA.E, PowellB.L, HallP.D, CaseL.D, Keittman R.J, Phase -1 trial of a novel diphtheria toxin/granulocyte macrophage colony-stimulating factor fusion protein (DT388GMCSF) for refractory or relapsed acute myeloid leukaemia.Clin.Oncol., 2002; 8: 1004-1013.
13. Seymour BLW, Ferry DR, Anderson D, Hesselwood S, Julyan P. J, Poyner R, et al, Hepatic drug targeting:Phase-1 evaluation of polymer-bound doxorubicin, j.Clin.Oncol., 2002; 20: 1668-1676.
14. Zhang W, Ran S, Sambade M, Huang X, Thorpe PE, A monoclonal antibody that blocks VEGF binding to VEGFR 2(KDR/Flk-1) inhibit vascular expression of Flk-1 and tumor growth in an orthotopic human breast cancer model, Angiogesis, 2002; 5: 35-44.
15. Noonberg SB, BenzCC, Tyrosine kinase inhibitors targeted to the epidermal growth factor receptor sub family: role as anticancer agents, Drugs, 2000; 59(4): 753-767.
16. Smith MR, Rituximab (monoclonal anti-CD 20 antibody): mechanism of action and resistance; Oncogene, 2000; 59(4): 753-767.
17. Leonard J.P,LinkB.K, Immunotherapy of non-Hodgkin's lymphoma with HLL-2(epratuzumab, an anti-CD22 monoclonal antibody) and HuID10 (apolizumab); Semen Oncol, 2002; 29(2): 81-86.

ANNEXURES

FTIR Spectroscopy of 5-Fu

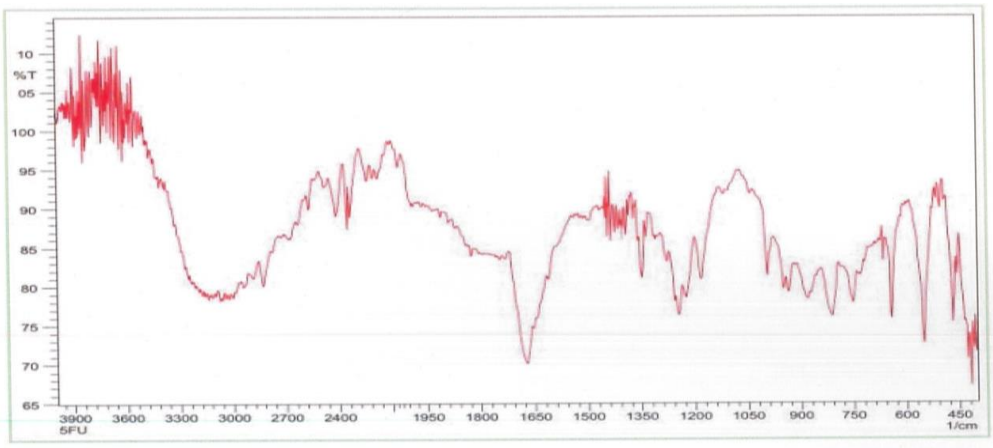

DSC data of 5- Fu

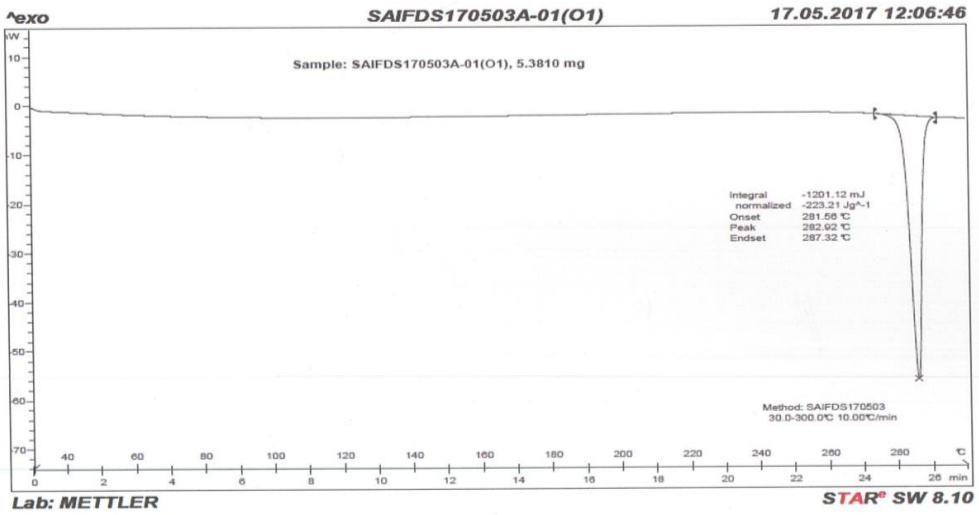

Powder of Diffraction of 5-Fu

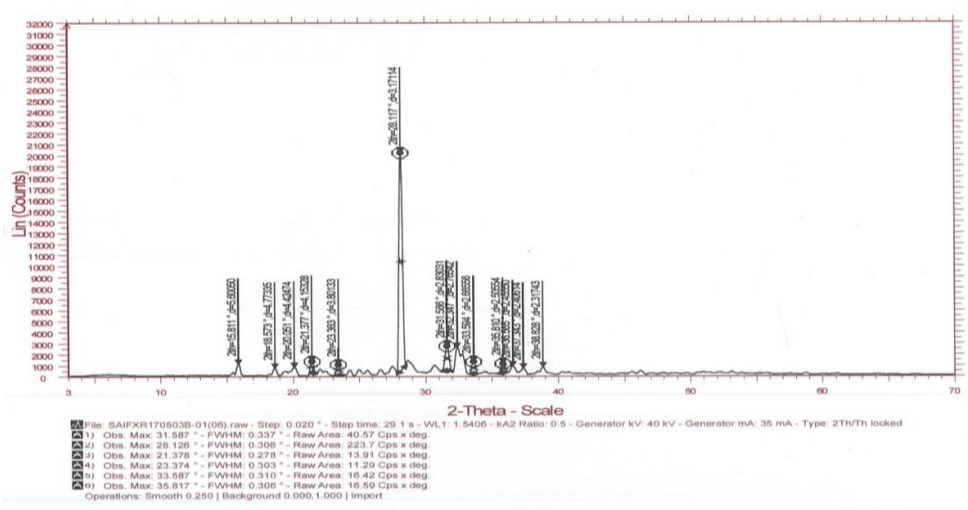

FTIR of PLGA

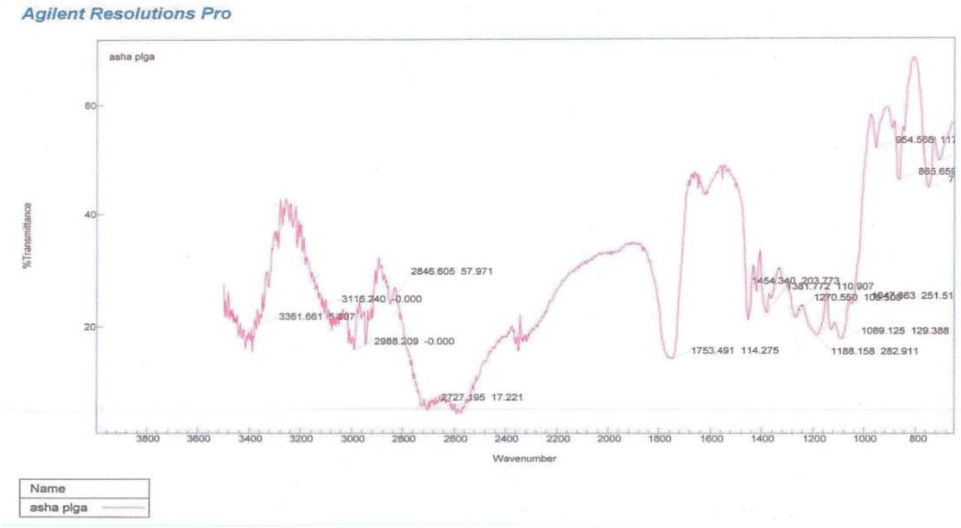

DSC of PLGA

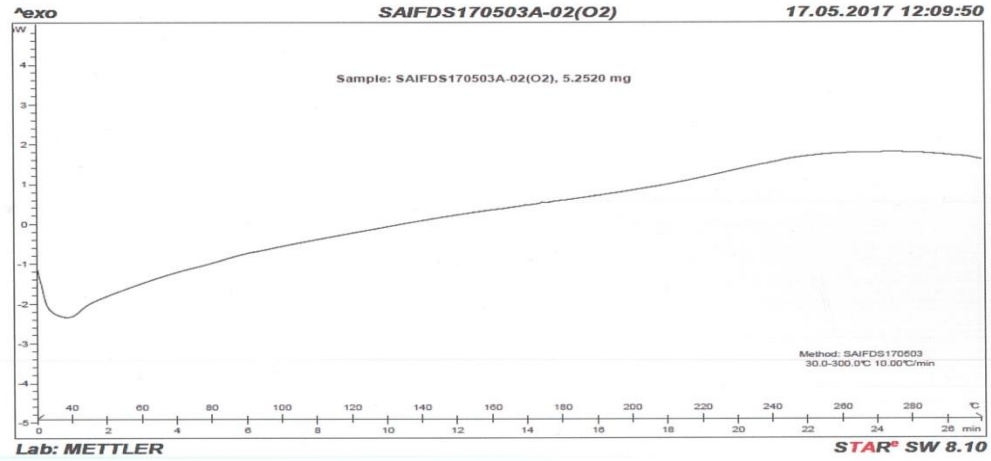

Powder X-ray Diffraction of PLGA

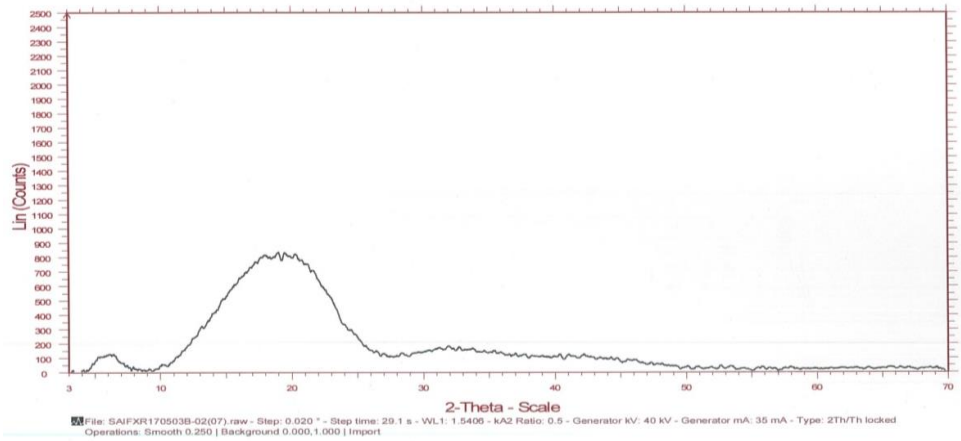

FTIR Spectroscopy of PEI

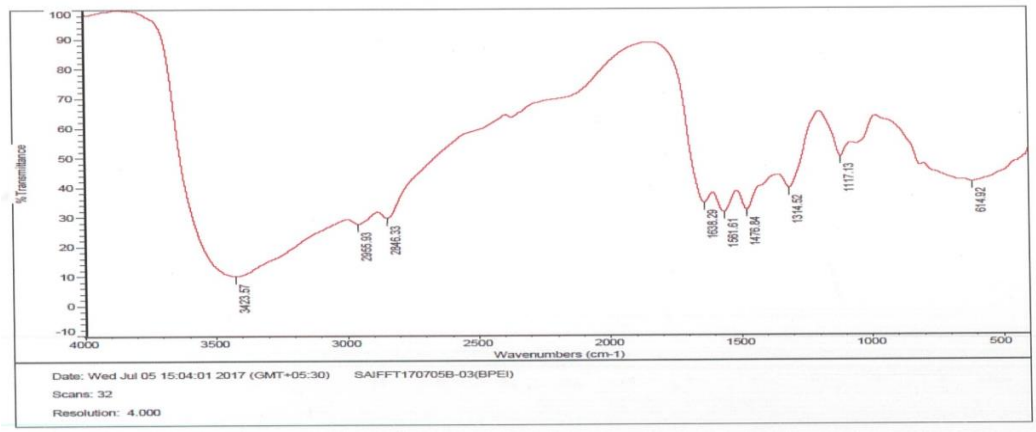

FTIR Spectroscopy of D-Biotin

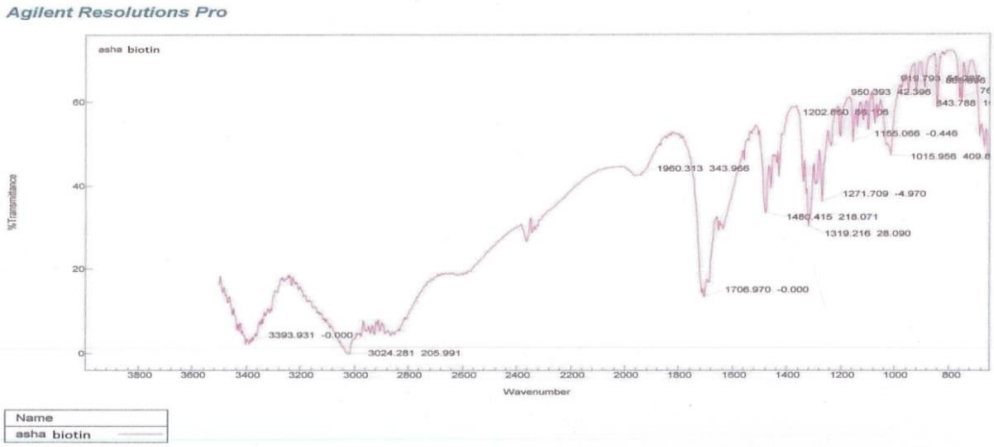

FTIR Spectro Scopy of PLGA- 5-Fu mixture

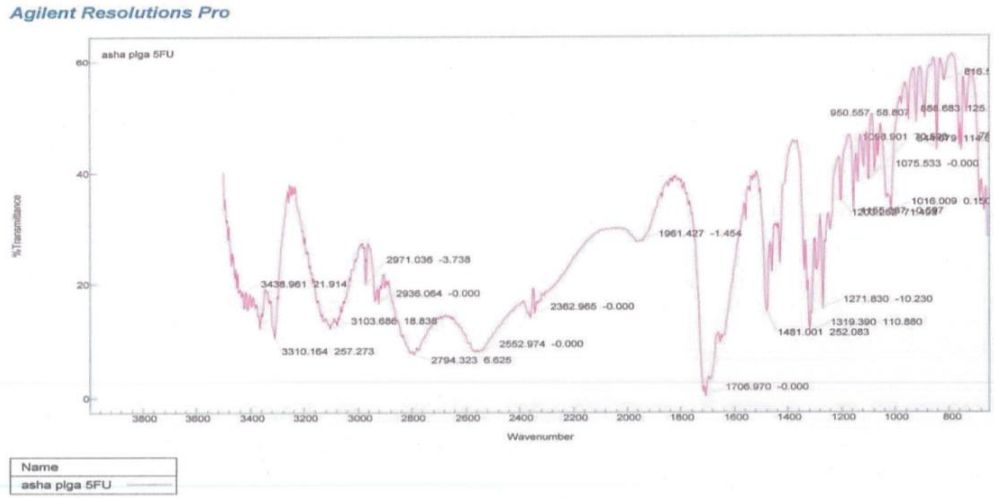

DSC of PLGA 5.Fu- Mixture

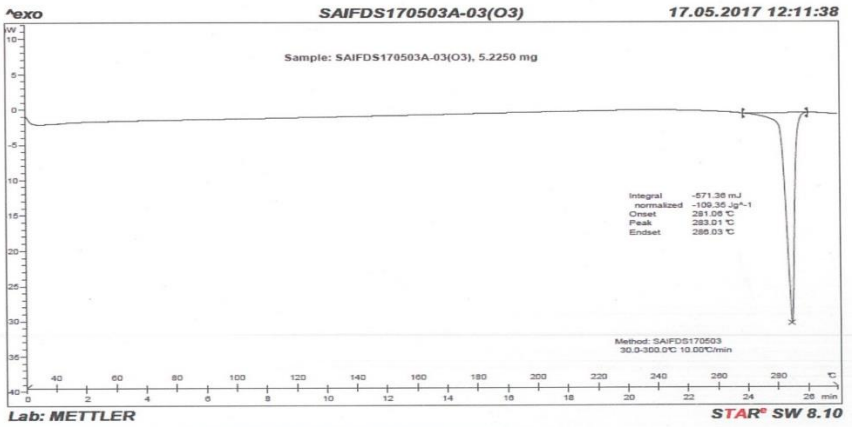

FTIR Spectroscopy of PLGA NPS

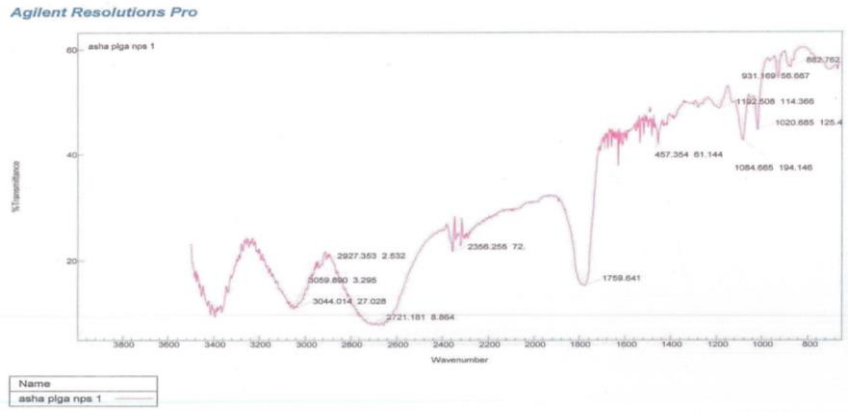

FTIR Spectro of Biotinylated Polyelthyleneimimines (BPET)

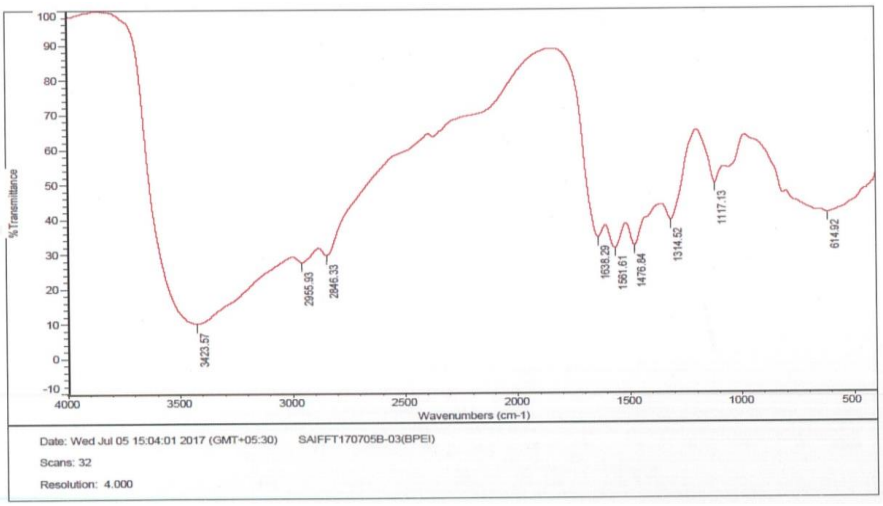

H^1 –NMR of BPEI

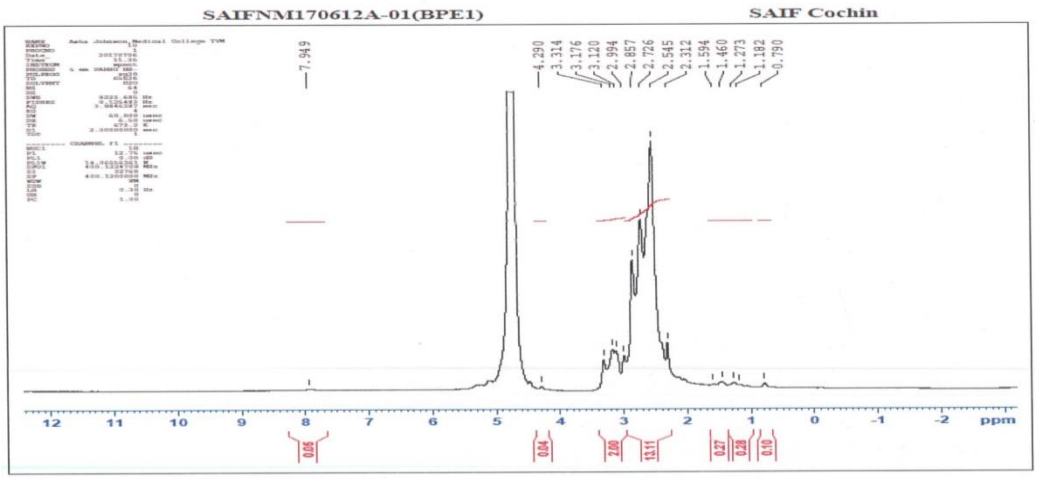

FTIR of Spectroscopy BPEI- NPS